

Scrambling under quench

Adith Sai Aramthottil¹, Diptarka Das², Suchetan Das² and Bidyut Dey²

(1) *Institute of Theoretical Physics, Jagiellonian University in Kraków, Łojasiewicza
11, 30-348 Kraków, Poland*

(2) *Department of Physics, Indian Institute of Technology - Kanpur,
Kanpur 208016, India*

2022/02/08

Abstract

We evaluate out of time ordered correlators in certain low dimensional quantum systems at zero temperature, subjected to homogenous quantum quenches. We find that when the Lyapunov exponent exists, it can be identified with the quenched energy. We show that the exponent naturally gets related to the post-quench effective temperature. In the context of sudden quenches the exponent is determined in terms of the quench amplitude while for smooth quenches we observe scalings of the exponent with the quench rate. The scalings are identical to that of the energy generated during the quench.

Contents

1	Introduction	2
2	Semiclassical chaos by differently ordered correlators	3
2.1	Sudden quench of the coupled oscillator	4
2.1.1	Numerics	5
2.2	Sudden quench in 2D CFT at large central charge	6
2.3	Smooth quench in the quantum Ising model	10
2.3.1	Numerical details	11
3	Conclusions	12
A	Details of tensor network for §2.3	15
A.1	DMRG	15
A.2	TDVP	15

1 Introduction

An ongoing activity of considerable interest is to investigate the physics out of equilibrium. While on one hand is the question about the late time fate of the non-equilibrium quantum state, on the other hand we want to uncover features in the dynamical evolution of the state. Under suitable conditions (e.g. eigenstate thermalization) the system equilibrates to certain ensembles characterized by a temperature and/or chemical potentials conjugate to the conserved charges. When energy is the only conserved quantity one expects the ensemble to be a thermal one, characterized by a temperature; to which all observables finally equilibrate. It is believed that a thermalizing non-equilibrium state also *scrambles*. Here the notion of scrambling is in the context of operator growth due to chaotic dynamics. This is suitably measured by the Lyapunov exponent () associated with the out of time ordered correlator (OTOC). In particular, for a maximally chaotic system in a thermal state, is proportional to the temperature. For an out of equilibrium state that is thermalizing, we therefore expect the dynamical to be related to the effective temperature to which this state equilibrates to. This temperature of course will depend on the energy generated during the quench, which further is governed by the particulars of the out of equilibrium scenario. Here we find evidences in some simple cases that the evaluated in the non-equilibrium state shows aspects commensurate with energy generation, which can indeed be associated with thermalization in certain cases.

The non-equilibrium scenario is generated by the set up of quantum quench; wherein some coupling in the Hamiltonian is changed as a function of time. Various kinds of universalities are known to be associated with investigations of quenches. These emerge most notably whenever adiabaticity gets broken. This is guaranteed if the change in coupling is either sudden or if it crosses a critical point. Typically in a theory with cut-off Λ , the initial state is characterized by a mass gap m_0 . The change of coupling $g(t)$ can be characterized by its rate of change, Γ and / or the change in the value of the coupling Δg .

For slow, smooth quenches in the regime, $\Gamma < m_0 < \Lambda$, the breakdown of adiabaticity is associated with the emergence of a Kibble-Zurek scale which imbues quenched correlation functions with universal scaling behaviours. There are also universal scalings expected in the fast regime, $\Lambda > \Gamma > m_0$ and in the sudden case $\Gamma \rightarrow 0$. Evidences for these scaling behaviours have been limited to holography, solvable lattice models, two dimensional conformal field theories (CFTs), free theories and certain large N theories. In this work, while remaining within this tractable set of illuminating theories we compute the OTOC during a quantum quench. Next, we outline the remaining sections along with the specific results from them.

In our first example we study the case of two harmonic oscillators x and y coupled by gx^2y^2 (see §2.1). This is a classically chaotic system, with classical

Lyapunov index given by $\lambda_{cl} \sim E^\nu$, where E is the classical energy. Interestingly, the quantum analog also exhibits a positive Lyapunov exponent $\lambda \sim T^\nu$ when the OTOC is computed in a thermal state with temperature T . The agreement with the classical exponent is not surprising as in the thermal quantum case, the typical energy is given by the temperature. We consider quenching at zero temperature the coupling g , suddenly and compute the generated energy. Through the energy we are able to ascribe an effective temperature in terms of Δg ; $T \sim (\Delta g)^\alpha$. Next, by computing the OTOC, we extract λ as a power of Δg which is consistent with the assigned effective temperature. The computations are carried out numerically, and although bound to errors due to various truncations, clearly illustrate that the OTOC prognosticates an effective thermalization resulting from the quench. In this set-up this statement is, $\lambda \sim (\Delta g)^{\nu\alpha}$.

The second example in §2.2 re-affirms the above observation of relating λ and Δg in a clean analytic example of sudden quench in 2D CFT in the limit of large central charge. We follow the Cardy-Calabrese prescription of approximating the quenched initial state with a regularized boundary state of the CFT. The regularization involves a parameter ϵ_0 which is directly related to the mass gap of the initial theory. We then implement the three point BCFT set-up, in the semi-classical regime, to extract $\lambda = \lambda(\epsilon_0)$. The parameter ϵ_0 is consistently related to the initial mass gap as well as the effective temperature of the quenched state.

The final example in §2.3 deals with the Ising chain in presence of both a transverse as well as a longitudinal field. We quench the transverse field smoothly (with rate Γ) while operating in a non-integrable regime. Under both the fast as well as slow quench, the quenched energy is known to scale differently as a function of Γ . We employ tensor network techniques to extract λ in this set-up and discover same scalings as for the energy generated during the quench.

All the three examples are indicative of the fact that in out of equilibrium scenarios where scrambling takes place, the Lyapunov exponent associated with suitable OTOCs can be identified with the energy generated. Furthermore, in scenarios where an effective post-quench temperature maybe estimated, the Lyapunov exponent is directly related with this temperature.

2 Semiclassical chaos by differently ordered correlators

Classical chaos is quantified by exponential sensitivity to initial conditions, which is given by the following Poisson bracket (P.B.) :

$$\frac{x(t)}{x(0)} = e^{\lambda_{cl}t} = \{x(t); p(0)\}_{P.B.}$$

The generalization in quantum mechanics is via different time commutators [1],

$$C = \langle [V(t); W(0)]^2 \rangle;$$

where the square is taken in order to prevent phase cancellations. When the commutator is expanded we find out of time ordered correlators of the form, $F(t) = \langle V(t)W(0)V(t)W(0) \rangle$, make up C . In particular for unitary hermitian operators $C = 2(1 - \text{Re}F(t))$. Therefore when C grows exponentially $\sim e^{2\lambda t}$ the quantity $F(t) \sim \text{const.} + \text{const.}'e^{\lambda t}$. The exponent λ has been shown to satisfy a universal bound set by the temperature when the expectation is evaluated in a thermal state. In our set-ups, instead of computing the OTOC in a thermal state we quench a zero temperature low lying quantum state of the initial Hamiltonian and extract the corresponding Lyapunov exponent.

2.1 Sudden quench of the coupled oscillator

For our first example we consider two coupled harmonic oscillators described by the Hamiltonian,

$$H = p_x^2 + p_y^2 + \frac{1}{4}(x^2 + y^2) + gx^2y^2; \quad (1)$$

Note that we avoid the simpler linear coupling, gxy , as via a global unitary transformation (in normal coordinates) the linear coupling problem can be reduced to two decoupled oscillators. This makes the model integrable, and OTOC only shows oscillatory behaviour with time.

Classically this has a non-zero λ which scales with energy as $\lambda \propto E^{1/4}$. In [2] the OTOC was computed in thermal state (temperature T) and it was found that $\lambda \sim T^c$ with $c \sim 0.25 - 0.31$. This is expected from the classical scaling since temperature plays the role of Energy. We compute the OTOC at zero temperature but under a sudden change of the coupling from g_0 to g . The quantity of interest is

$$C = -\langle n_0 | [x(t); p(0)]^2 | n_0 \rangle; \quad (2)$$

where $|n_0\rangle$ is a low lying energy eigenstate of the initial Hamiltonian $H(g_0) = H_0$. The time evolved position operator $x(t)$ is calculated with the quenched Hamiltonian $H(g)$: $x(t) = \exp(itH(g))x(0)\exp(-itH(g))$. We evaluate C by inserting complete set of eigenstates of the new Hamiltonian $H(g)$ that we denote as $|m\rangle$.

$$C = -\sum_m \langle n_0 | [x(t); p(0)] | m \rangle \langle m | [x(t); p(0)] | n_0 \rangle = \sum_m b_m(t)b_m^*(t); \quad (3)$$

the quantity $b_m(t) = -i\langle n_0 | [x(t); p(0)] | m \rangle$ is Hermitian. Using another set of completeness insertions and the relation between matrix elements of p and x :

$\rho_{km} = \frac{i}{2} E_{km} \chi_{km}$ we find :

$$b_m(t) = \frac{1}{2} \sum_{l,k} \langle n_0 | l \rangle \chi_{lk} \chi_{km} (E_{km} e^{iE_{lk}t} - E_{lk} e^{iE_{km}t}) : \quad (4)$$

Here, $\chi_{km} = \langle k | x | m \rangle$ and $E_{km} = E_k - E_m$. This is the main quantity that we compute numerically, which is plugged into eq(3) to get the OTOC. The wavefunctions $\langle x; y | n \rangle = \psi_n(x; y)$ are obtained by solving the Schrödinger's equation:

$$-\left(\frac{\partial^2}{\partial x^2} + \frac{\partial^2}{\partial y^2}\right) \psi_n(x; y) + \left(\frac{1}{4}(x^2 + y^2) + gx^2y^2\right) \psi_n(x; y) = E_n \psi_n(x; y); \quad (5)$$

with Dirichlet (wavefunction vanishing) boundary conditions in a square box.

2.1.1 Numerics

The equation (5) is solved for various values of the coupling g that is relevant to us. The `Mathematica`[®] package `NDEigensystem` has been used to get the wavefunctions. The initial state $|n_0\rangle$ is taken to be a low lying eigenstate of H_0 . The box size is kept at 20×20 . The energy levels are suitably truncated in the completeness relations. Once the wavefunctions $\psi_{n_0}(x; y)$ and $\psi_m(x; y)$ corresponding to H_0 and $H(g)$ respectively are available, we numerically integrate using the `NIntegrate` command to find the overlaps and the matrix elements as needed in (4). We show the behaviour of C as a function of time for different changes in amplitude of the coupling, $\Delta g = g - g_0$, in Fig. 1. Also as can be seen in the figure, when the quench amplitude is very small then $C(t)$ does not have any exponential growth. All the plots have a regime where $C(t)$ grows exponentially with time, before beginning to oscillate in some complicated manner. Fortunately, the early time behaviour is sufficient to extract a Lyapunov exponent λ , since in any case due to truncation of high energy levels, late time numerics is unreliable. To extract the Lyapunov exponent we fit $C(t)$ for different values of Δg with $b \exp(2 \lambda t)$. Next we plot λ as a function of Δg and find that $\lambda \sim (\Delta g)^\theta$. In Fig. 2, we present the case when the initial state is the 10th eigenstate, for which the exponent turns out to be close to 0.25. For other initial states as well, we find numerical fits for the exponent to be close to a quarter. In the thermal ensemble $\lambda \sim T^c$ with c extracted from a similar numerical regime and fitted to similar values. Therefore, this is encouraging as it suggests, that Δg seems to play the role of temperature.

It turns out that there is further evidence for this ‘‘thermal’’ interpretation of Δg . We extracted an effective temperature for a given Δg by equalizing energy computed in the thermal ensemble of H_0 and that in the quenched state, *i.e.* we solve for T from the equation:

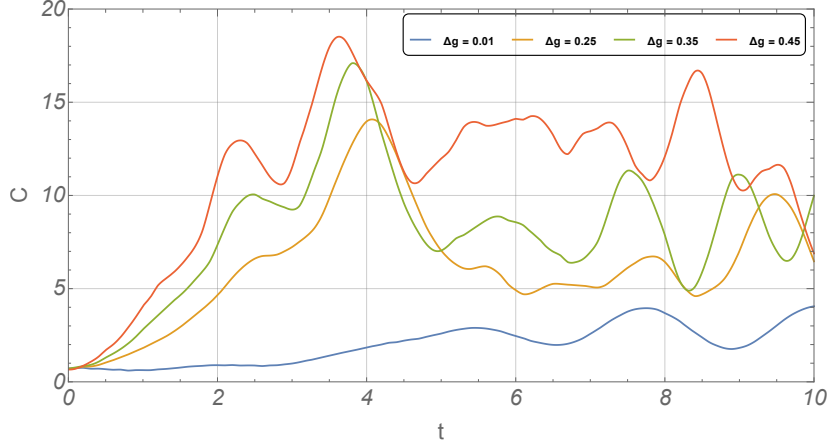


Figure 1: The time development of the commutator squared value shown for different quench amplitudes.

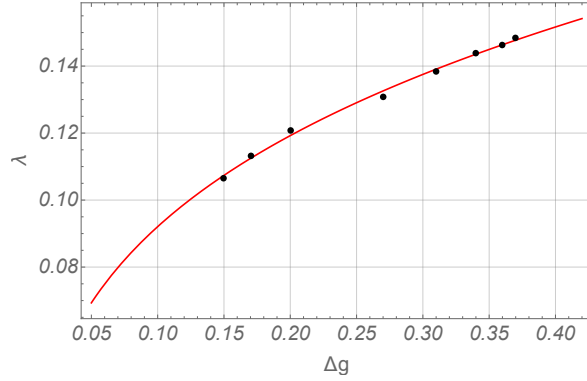


Figure 2: We fit the extracted λ values (black) to $a + b(\Delta g)^\theta$ (red curve). When we restrict $\theta \in [0;1;0;4]$ the best fit is obtained for $\theta = 0;255$.

$$\langle H_0 \rangle_T = \frac{\sum_{k_0} E_{k_0} e^{-E_{k_0}/T}}{\sum_{j_0} e^{-E_{j_0}/T}} = \sum_m E_m |\langle n_0 | m \rangle|^2 \quad (6)$$

The R.H.S contains the information about the quench and uses numerical results that we already used to compute $b_m(t)$. In Fig. 3 we plot the effective temperature as a function of Δg and obtain a straight line, this therefore strengthens our thermal explanation for the scaling of the Lyapunov exponent.

2.2 Sudden quench in 2D CFT at large central charge

In this section we study the OTOC for sudden critical quenches in one spatial dimension. The initial state $|0\rangle$ is the ground state of a gapped Hamiltonian, with gap $\sim 1 = \epsilon_0$. At time zero, the gap is closed suddenly as the Hamiltonian changes

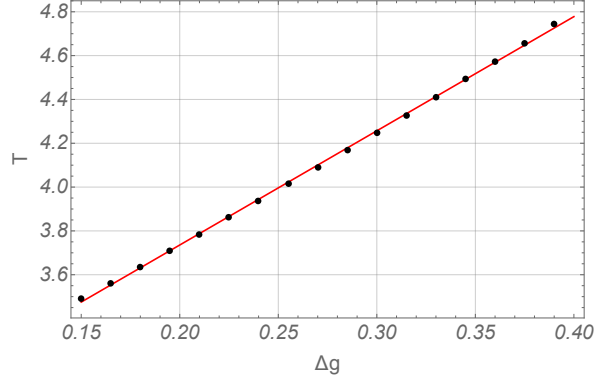


Figure 3: The effective temperature fits linearly with the quench amplitude.

to H_{CFT} . From the perspective of the conformal theory, there is a boundary at Euclidean zero time, which is naturally associated with a boundary state of the CFT. Since in the infrared this state should be a conformal boundary state $|\mathbf{B}\rangle$, a good approximation to $|0\rangle$ is provided by an irrelevant deformation to $|\mathbf{B}\rangle$. The lowest universal irrelevant operator is a single power of the Hamiltonian itself. This is the proposed prescription of Cardy and Calabrese (CC) [3,4] :

$$|0\rangle \propto e^{-\tau_0 H} |\mathbf{B}\rangle \quad (7)$$

Note, that the RG distance between $|0\rangle$ and $|\mathbf{B}\rangle$, which is, $1/\text{gap} = \tau_0$ acts also as a regularizing parameter for the non-normalizable boundary state. Thereafter, post critical quench observables can be calculated as Euclidean strip (of width $2\tau_0$) correlators, which are suitable analytically continued to get the Lorentzian answers. The correlators of primary fields $\phi_i(x_i; \tau_i)$ ($i = 1; 2; \dots; n$) in the strip can be mapped to that on upper half plane(UHP) using the following conformal transformation

$$\tau \rightarrow z = i e^{\frac{\pi\omega}{2\tau_0}}; \tau = x + i \tau \quad (8)$$

This mapping allows us to relate:

$$\left\langle \prod_{i=1}^n \phi_i(\tau_i; \tau_i) \right\rangle_{\text{strip}} = \prod_{i=1}^n \tau_i^{-h_i} \tau_i^{-\bar{h}_i} \left\langle \prod_{i=1}^n \phi_i(z_i; \bar{z}_i) \right\rangle_{\text{UHP}} \quad (9)$$

Here $(z; \bar{z})$ are UHP coordinates. Two or higher point functions are not fixed on the UHP, as using the conformal ward identities one can show that n -point BCFT correlators are equivalent to $2n$ -point holomorphic CFT correlators on the entire plane. One point functions, however get fixed. An important one point function is the expectation value of the post-quench energy : $\langle 0|H_{CFT}|0\rangle$. The contribution comes only from Schwarzian derivative associated with the map (8).

$$\langle \mathbf{B} | e^{-\tau_0 H_{CFT}} H_{CFT} e^{-\tau_0 H_{CFT}} | \mathbf{B} \rangle = \frac{c}{96} \frac{2}{\tau_0} \quad (10)$$

This result can also be obtained from the T_{00} expectation value in a thermal ensemble with inverse temperature $\beta = 4 \ell_0$, since

$$\frac{\text{tr}(H_{CFT} e^{-\beta H_{CFT}})}{\text{tr}(e^{-\beta H_{CFT}})} = \frac{c}{6 \ell_0^2}.$$

Hence, the quench gap / energy gets naturally associated to an effective temperature.

Extracting the Lyapunov exponent from BCFT

In [5], the authors used a certain three point bulk-boundary thermal OTOC which shows maximal Lyapunov behaviour in large central charge limit of the BCFT. Here we consider three operators placed in the following way. W of dimension h_w is sitting at $(x; 0)$ and two boundary operators V of dimensions h_v are sitting at $(0; t)$ in the Lorentzian coordinate. The OTOC can be obtained from the following object:

$$C(t) = \frac{\langle V(t)W(0)V(t) \rangle}{\langle W \rangle \langle VV \rangle} \quad (11)$$

Operationally, to get the above out of time ordered object from the Euclidean correlator (with all operators O_i at Euclidean time τ_i), we analytically continue the τ_i 's to their original Lorentzian values *i.e.* $\tau_i = t_i + i \epsilon_i$. Ultimately, we take all $\epsilon_i \rightarrow 0$ and the ordering in time comes from the ordering of the taking the limits of different τ_i 's.

Using once again the map (8) the Euclidean correlator, C_E is equivalent to a four point holomorphic function on the full plane, since only the bulk operator W gets mirrored on the lower half plane. C_E is just a function of the Euclidean cross-ratio Z , and in the complex Z plane possesses branch-cuts originating from points when operators enter into each others' light cones. After analytic continuation, different time ordering dictates how or whether the branch cuts are being crossed. Here in our case, the four points on the plane, after the analytic continuation, are the following:

$$z_0 = i e^{b(x+i\epsilon_0)}; \bar{z}_0 = -i e^{b(x-i\epsilon_0)}; z_1 = i e^{b(t+i\epsilon_1)}; z_2 = i e^{b(t+i\epsilon_2)}; b = \frac{c}{2 \ell_0}. \quad (12)$$

Here we take $\epsilon_1 = \epsilon_0$ and $\epsilon_2 = -\epsilon_0$ such that z_1 and z_2 are placed on the boundary of the UHP. Hence the cross ratio Z is given by $Z = \frac{(z_0 - \bar{z}_0)(z_1 - z_2)}{(z_0 - z_1)(\bar{z}_0 - z_2)}$. For different time regimes, we get the following asymptotic behaviours for the cross-ratio:

$$\begin{aligned} Z_{t \rightarrow 0} &= \frac{2i \frac{c}{12}}{e^{bx} - e^{-bx}}; \quad Z_{t \gg x} = -2i \frac{c}{12} e^{-b(t-x)}; \\ Z_{t=x} &= -\frac{2i \frac{c}{12}}{(1 - e^{ib(\epsilon_0 - \epsilon_1)})(1 + e^{-ib(\epsilon_0 + \epsilon_1)})} \approx \frac{c}{10}. \end{aligned} \quad (13)$$

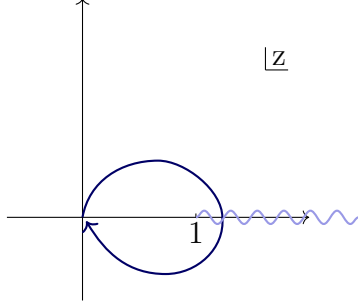


Figure 4: During the analytic continuation for OTOC the cut from 1 to infinity is crossed.

Here we have defined $\epsilon_{ij} \equiv i(e^{ib\epsilon_i} - e^{ib\epsilon_j})$ and ϵ_{ij}^* is the corresponding complex conjugate. From the above analysis, we see that the cross ratio goes to zero from opposite direction at $t \rightarrow 0$ and $t \rightarrow \infty$ limit and this is independent of the ϵ_i ordering. However at $t = x$, the cross ratio shows interesting behavior since it is a ratio of ϵ_{ij} s. In particular for the OTOC, we need the following ordering: $\epsilon_{10} > \epsilon_{02} > \epsilon_{20}$. In this case, from (13) we could clearly see that $Z_{t=x} \approx 1 + \frac{\epsilon_{02}^*}{\epsilon_{10}^*} > 1$. Diagrammatically the situation is described in the figure (4).

In the large central charge limit, we may assume that the dominant contribution to $C_E(z)$ comes from the Virasoro identity block, $\mathcal{F}(z)$ which in the monodromy regime of $h_i=c$ fixed with: $h_v \ll h_w$ has the universal form:

$$\mathcal{F}(z) \approx \left(\frac{z}{1 - (1-z)^{1-12\frac{h_w}{c}}} \right)^{2h_v} \quad (14)$$

To get to our desired OTOC, we need to wind around the branch cut at $z = 1$ and then as Lorentzian time increases, end up at small $|z|$. Therefore we implement $(1-z) \rightarrow (1-z)e^{2\pi i}$ and then expand in small z , which leads to:

$$\mathcal{F}(z) \approx \left(\frac{1}{1 - \frac{24i\pi h_w}{cz}} \right)^{2h_v} \quad (15)$$

In terms of the Lorentzian time, t :

$$C(t) \approx \left(\frac{1}{1 + \frac{12\pi h_w}{\epsilon_{12}^*} e^{b(t-t_*-x)}} \right)^{2h_v} : \quad (16)$$

In the above expression, the scrambling time $t_* = \frac{1}{b} \log(c)$ and the Lyapunov exponent associated with $C(t)$ is

$$= b = \frac{2}{0} \quad (17)$$

Comparing with the maximal Lyapunov exponent for the large c thermal OTOC ($2/T$), we once again get the effective inverse temperature to be $\beta = 4/\beta_0$. Once again, we see that the effective temperature associated with the quantum quench determines the scrambling behaviour. This result has also been obtained recently in [6].

2.3 Smooth quench in the quantum Ising model

We now explore the identification of the Lyapunov index with the energy generated during quench in the canonical quantum Ising chain. Intense quenching investigations has been carried out in this many-body lattice model. In particular, results exist for behaviour of the energy generated for smooth quenches. There are two distinct scaling regimes for smooth quenches, *viz.* the slow or the Kibble-Zurek (KZ) regime [7] and the fast regime [8]. They are separated by the mass-gap scale of the initial Hamiltonian. While KZ can be understood using the diabatic approximation, the fast scaling can be derived by using conformal perturbation theory.

The quantum Ising model in one spatial dimensions is described by

$$H = - \sum_i J Z_i \otimes Z_{i+1} + g X_i + \Gamma Z_i: \quad (18)$$

We turn on both a transverse as well as an infinitesimal longitudinal field in order to be in the non-integrable regime. When the longitudinal field is absent, fermionization takes the model to a free massive ($m \propto 1 - |g=J|$) fermionic theory which is integrable. We quench linearly the coupling $g = g_0 + \Gamma t$ which plays the role of the transverse magnetic field. The Pauli X is bilinear in terms of the Jordan-Wigner fermions, $\bar{\psi} \psi$ and has scaling dimension $\Delta = 1$, which is also the dimension of the energy operator. For relativistic theories in the KZ regime ($\Gamma < m$), one-point functions, $\langle O_\Delta \rangle \sim t_{KZ}^{-\Delta}$. Here t_{KZ} is determined from the adiabaticity breakdown condition. For the Ising model $t_{KZ} \sim \Gamma^{-1/2}$. Therefore the energy generated in the KZ regime is expected to show a $\sqrt{\Gamma}$ scaling.

The fast scaling regime is naturally defined by $\Lambda_{UV} > \Gamma > m$. Since the theory is insensitive to any scales other than the UV cut-off, it is approximately conformal. Therefore $\langle O_\Delta \rangle \sim \Gamma^{2-2\Delta}$. Thus the energy generated shows logarithmic scaling with Γ . During smooth quenches of the transverse field Ising model, these scaling laws were showcased in the $\langle \bar{\psi} \psi \rangle$ operator expectation value [9].

Here, we compute the OTOC in the ground state of the initial $H(g_0)$:

$$C(t) = \langle 0 | Z_j(t) Z_j(0) Z_j(t) Z_j(0) | 0 \rangle: \quad (19)$$

Note, that we choose the Z Pauli matrices since these are non-local in terms of the Jordan-Wigner fermions and have been shown (i) to exhibit “fast” thermalization and, even in the integrable regime, (ii) to mimic exponential Lyapunov behaviour

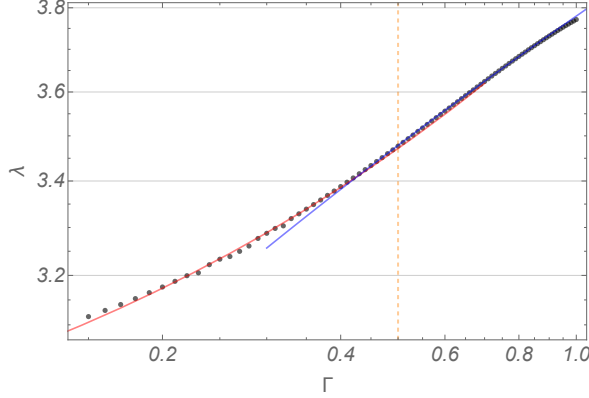


Figure 5: The Lyapunov exponent as a function of the quench rate Γ , shows $\sqrt{\Gamma}$ scaling (red is fit to $a_1 + a_2\sqrt{\Gamma}$) in the KZ regime which smoothly goes over to $\log\Gamma$ scaling (blue is fit to $a_1 + a_2 \log \Gamma$) in the fast regime. The orange dashed line demarcates the two regimes.

in thermal state [10]. We find that the extracted Lyapunov exhibits the same smooth quench scalings as the energy generated, see Fig. 5. This once again strongly indicates that scrambling gets related to effective thermalization, and in fact that the energy generated via quench can be interpreted as the ‘heat’ generated [11, 12].

2.3.1 Numerical details

The OTOC has been evaluated with the help of tensor network (TN) techniques, see §Appendix A for further details. This allows us to go upto system size $L = 50$. We have chosen periodic boundary conditions on the chain, and computed OTOC for Pauli Z operators at the middle = 25th site. The parameters used for the numerics are: $g_0 = 0.5; J = 1; \epsilon = 0.0001$. Starting with the ground state in the ferromagnetic phase, we evolve the state with the time-dependent Hamiltonian, for different rates : $\dot{g} = \Gamma$. Numerically we implement this by discretizing the time-step in units of $\delta t = 0.01$. In the Schrödinger picture the OTOC can be represented as

$$\text{OTOC}(t) = \langle _0 | Z_{25} \mathcal{U}(-t) Z_{25} \mathcal{U}(t) Z_{25} \mathcal{U}(-t) Z_{25} \mathcal{U}(t) | _0 \rangle \quad (20)$$

where the evolution operator is of the form $\mathcal{U}(t) = e^{-i\mathcal{H}(g(t))\delta t} \dots e^{-i\mathcal{H}(g_0)\delta t}$. As described in the appendix since we use time-dependent variational principle algorithm (TDVP), the tensor network also gets optimized during the time-evolution. See Fig. 7 for a schematic of the contracted network used to extract the OTOC.

Since the OTOC is for Hermitian operators, we extract the squared commutator using: $C(t) = 2(1 - \text{Re}(\text{OTOC}(t)))$. For the quenches we observe $C(t)$ to behave similar to that of the coupled oscillator quench Fig. 1, there is a

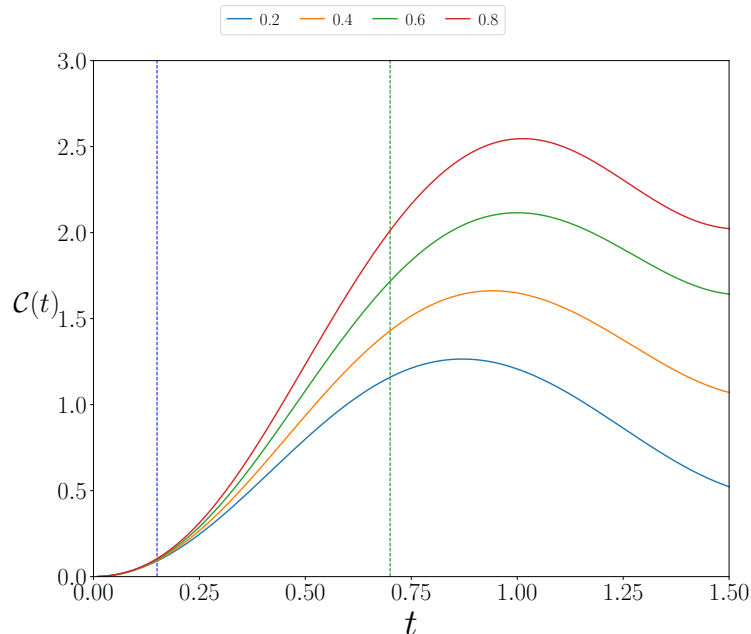


Figure 6: The time development of the commutator squared value shown for different rates of quench.

clear transient period where the commutator squared grows exponentially before starting to oscillate, see Fig. 6. Fortunately for us, the OTOC characterization is for very early times, and thus we do not have to deal with the growing entanglement at late times which acts as a bottleneck for the TN techniques owing to finiteness of the bond dimension. As shown in the figure, we extract by fitting an exponential between $0:15 \leq t \leq 0:70$, for different rates. From this data we find the scaling shown in Fig. 5.

In theories like the Ising model, operators have bounded norms. Therefore only transient chaotic behaviour is observable, since the bounds get saturated very soon. This motivates the consideration of density of OTOCs of extensive sums of local operators, which can show longer regimes of scrambling behaviour [13]. We expect that the scaling behaviours observed in the Lyapunov exponent also to hold even in these modified OTOCs.

3 Conclusions

In this work we have studied scrambling during quantum quenches. All the chosen models start from a gapped low lying eigenstate of an initial Hamiltonian and then during the quench evolution either gets coupled to another system, or experiences sudden criticality, or evolves with a smoothly changing coupling. In

all the situations, for suitably chosen operators, signs of scrambling in the form of exponential OTOCs are observed. The extracted Lyapunov exponents have the characteristics of an effective temperature since it can be identified with the energy generated during the quench. Furthermore in the case of smooth quenches the extracted Lyapunov exhibits both a Kibble-Zurek as well as a fast scaling as expected in the quench energy.

The coupled oscillator studied in this work can be shown to arise from the dimensional reduction of $SU(2)$ Yang-Mills Higgs theory in the unitary gauge [2]. In the thermal context the scaling of the Lyapunov index with the temperature is expected to hold for the full Yang-Mills as well as its susy generalizations. A very interesting generalization is the $SU(N)$ Yang-Mills in $9 + 1$ dimensions with large N . When dimensionally reduced to zero dimensions, it is described by D0-brane matrix quantum mechanics. At high temperatures the Lyapunov index of this matrix model also shows the scaling $\sim T^{1/4}$ [14, 15]. It is then expected that the OTOC during a quench in these generalizations will also exhibit scalings. Using the gauge/gravity correspondence this will translate to universal scalings in genuinely non-equilibrium quantum gravity processes, which may include black hole formations as well as black hole transitions. It is to be noted, that equilibration after quenches have already been studied in various matrix models [16].

As pointed out here as well as in [2], the exponent of $1/4$ has its origin in the behaviour of the classical Lyapunov exponent. However the Lyapunov index extracted from the OTOC can be distinct from the classical Lyapunov exponent in certain physical systems as shown in [17, 18]. Hence, it will be quite interesting to carry out the quench and investigate the nature of effective thermalization as determined from scrambling in these models.

In the context of the gauge/gravity duality, universal scalings of quenched correlation functions in the field theory can be understood from bulk zero mode dynamics in the dual gravity theory [19]. On the other hand, OTOCs in holography can be computed from the bulk using a shockwave set-up [20]. It will thereby be interesting to imbue the end of world brane geometry (dual to the Cardy-Calabrese quenched state [21]) with shockwaves and investigate the role of zero modes in the Lyapunov scalings.

A common underlying theme in our examples is the emergence of a scale through an effective “thermalization”. It is a natural question to ask what happens to the Lyapunovian behaviour when there are additional conserved charges? In this case one expects the final state to equilibrate to a generalized Gibbs ensemble, with generically non-zero chemical potentials turned on for different charges. For a CFT with an additional global $U(1)$ scrambling has been explored in the context of local quenches [22]. We expect that signs of such effective equilibration will get reflected in the scrambling characterizations associated with quenches.

When there are as many conserved charges as the degrees of freedom, a the-

ory becomes integrable. Integrable theories are known not to show exponential OTOCs, however in presence of non-integrable perturbations can have a rich phase diagram of Lyapunovian dynamics, as was shown using the quantum tangent space formalism in [23]. Though our analysis of the Ising model falls in this class, it will be interesting to explore more generally within this framework the case of scrambling under quench.

In context of time-dependence and the quantum Ising model, OTOCs have also been explored in [24] and very recently in [25]. While the former establishes OTOCs as an order parameter during sudden quenches,¹ the latter shows how the information about dynamic phase transitions are present in the OTOC corresponding to non-local operators. Both these studies are based on late-time properties of the OTOC, whereas our investigation is complementary since it focuses on the early time behaviour. It will also be interesting to explore scrambling during smooth quenches in models with richer critical structures and also in presence of *disorder*, e.g., [27].

Recently TN + Prony method has been used in the non-integrable Ising model at finite temperature to compute unequal time commutators [28] with some success. It seems only natural to adapt these techniques to explore non-equilibrium scrambling in future.

It will also be interesting to explore OTOCs in quenches for analytically controllable interacting field theories. At finite temperatures both in the $O(N)$ non-linear sigma model [29] as well as the Gross-Neveu model [30] the Lyapunov exponent scales linearly with temperature at large N . Furthermore, the Schwinger-Keldysh formalism for studying quantum quenches have already been explored in these models [31, 32].

Note Added :

While this work was nearing completion, the recent preprint [6] has explored OTOCs during inhomogenous quenches in the context of two dimensional CFTs, wherein they also independently obtained (17).

Acknowledgements

It is a pleasure to thank Titas Chanda, Amit Dutta, Bobby Ezhuthachan, Michal P. Heller, Arijit Kundu and Arnab Kundu for several useful discussions. DD, SD, & BD would like to acknowledge the support provided by the Max Planck Partner Group grant MAXPLA/PHY/2018577. DD would also like to acknowledge the support provided by the MATRICS grant SERB/PHY/2020334. ASA would like to thank Titas Chanda for Tensor Network codes. ASA would like to acknowledge the support provided by National Science Centre (Poland) under

¹Assuming eigenstate thermalization this late time behaviour follows very naturally, see [26].

project 2019/35/B/ST2/00034. BD would like to thank Supratim Das Bakshi for useful comments on Mathematica code. BD also acknowledges MHRD, India for Research Fellowship.

A Details of tensor network for §2.3

The low lying initial state before the quench was achieved using Density Matrix Renormalization Group(DMRG). And the time-evolution in the OTOC was done using the recently developed time-dependent variational principle (TDVP) [33–35]. The MPSs and Matrix Product Operators in the entire Tensor Network calculations have been constructed using ITensor C++ library (<https://itensor.org>).

A.1 DMRG

Here we use the strictly single site DMRG(DMRG3s) [36] from an initial random matrix product state(MPS) of bond-dimension $\chi = 10$, to approach a low lying state. This is then followed with an application of single-site DMRG. We use DMRG3s initially as it avoids getting stuck in local minimas which is the case with single-site DMRG.

A.2 TDVP

For an initial MPS state $|\Psi(\mathbf{A})\rangle$ the time evolution using TDVP can be understood as an orthogonal projection of the evolution vector of the Schrödinger equation onto the tangent space of the present MPS manifold numerically restricted by dimension

$$\frac{d|\Psi(\mathbf{A})\rangle}{dt} = -i\hat{\mathcal{P}}_{\mathcal{M}_{MPS_\chi}} \mathcal{H}|\Psi(\mathbf{A})\rangle \quad (21)$$

where $\mathcal{P}_{\mathcal{M}_{MPS_\chi}}$ is the projector that maps $\Psi(\mathbf{A})$ to the tangent space of the MPS manifold of dimension χ . We follow the prescription of [34,37] to implement the one-site and 2-site TDVPs. For initial times until we reach the maximum bond dimension $\chi = 256$ we do the TDVP evolution with 2-site TDVP as this helps in extending the bond dimension, this is shown in FIG. 7. If the maximum bond dimension is reached we switch to single-site TDVP (this is not expected as the time evolution of each Hamiltonian is only for short periods). Note that unlike the traditional use of TDVPs which evolve the state over a time t with discrete steps Δt , we make an evolution over a very short period $\Delta t = 0:01$, then change the g value in the Hamiltonian and make a short TDVP evolution again. This step is repeated until the desired value of time is reached. The value of Δt is taken to be small not because of the error incurred as it has been previously shown

that steps smaller than $\epsilon = 0.1$ with properly converged Lanczos exponentiation do not affect the evolution [38], but rather to have more OTOC values in the desired transient interval.

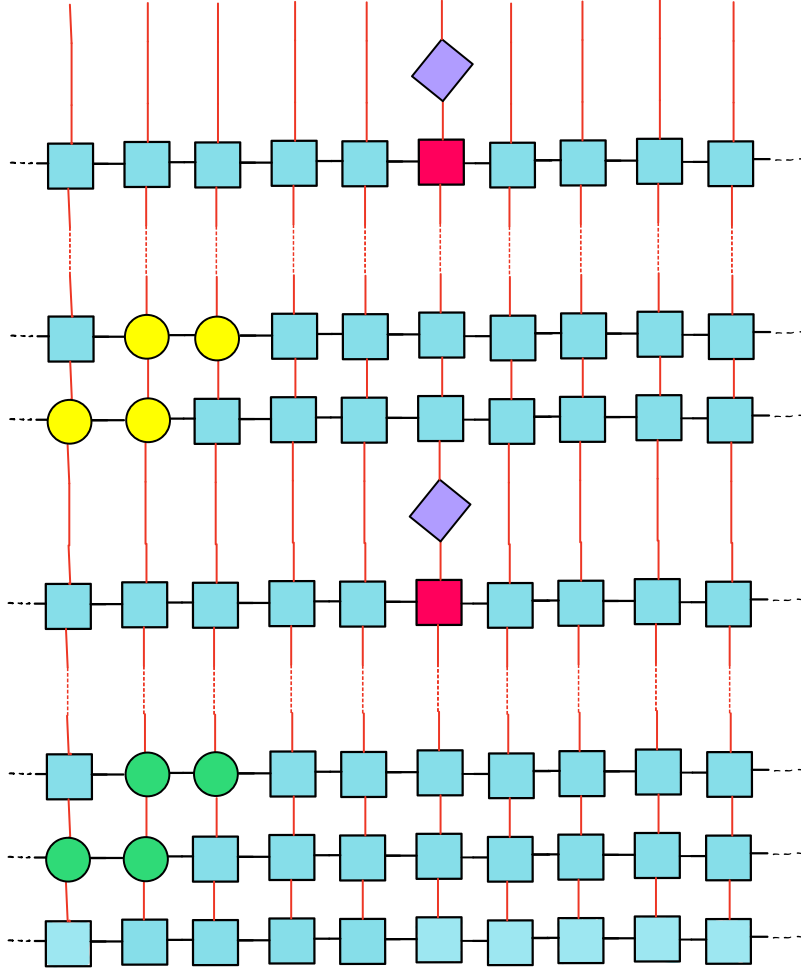


Figure 7: The green and yellow tensors denote the two-site centers of the mixed canonical form for the forward and backward time evolution respectively. This changes with sweeps left to right and right to left [37]. The sweeps on the network depends on the instantaneous Hamiltonian. Each layer depends on the instantaneous Hamiltonian. After time evolution to the desired time, the central site is made the one-site center of the mixed canonical form (red tensor) and acted on with Z_{25} which is denoted by the violet tensor.

References

- [1] B. Swingle, *Unscrambling the physics of out-of-time-order correlators*, *Nature Phys.* **14** (2018) 988. 4
- [2] T. Akutagawa, K. Hashimoto, T. Sasaki and R. Watanabe, *Out-of-time-order correlator in coupled harmonic oscillators*, *JHEP* **08** (2020) 013 [2004.04381]. 4, 13
- [3] P. Calabrese and J.L. Cardy, *Time-dependence of correlation functions following a quantum quench*, *Phys. Rev. Lett.* **96** (2006) 136801 [cond-mat/0601225]. 7
- [4] P. Calabrese and J. Cardy, *Quantum quenches in 1 + 1 dimensional conformal field theories*, *J. Stat. Mech.* **1606** (2016) 064003 [1603.02889]. 7
- [5] S. Das, B. Ezhuthachan and A. Kundu, *Real time dynamics from low point correlators in 2d BCFT*, *JHEP* **12** (2019) 141 [1907.08763]. 8
- [6] S. Das, B. Ezhuthachan, A. Kundu, S. Porey and B. Roy, *Critical quenches, otocs and early-time chaos*, **2108.12884**. 10, 14
- [7] A. Polkovnikov, K. Sengupta, A. Silva and M. Vengalattore, *Colloquium: Nonequilibrium dynamics of closed interacting quantum systems*, *Rev. Mod. Phys.* **83** (2011) 863. 10
- [8] S.R. Das, D.A. Galante and R.C. Myers, *Quantum Quenches in Free Field Theory: Universal Scaling at Any Rate*, *JHEP* **05** (2016) 164 [1602.08547]. 10
- [9] D. Das, S.R. Das, D.A. Galante, R.C. Myers and K. Sengupta, *An exactly solvable quench protocol for integrable spin models*, *JHEP* **11** (2017) 157 [1706.02322]. 10
- [10] C.-J. Lin and O.I. Motrunich, *Out-of-time-ordered correlators in a quantum ising chain*, *Physical Review B* **97** (2018) . 11
- [11] C. De Grandi, V. Gritsev and A. Polkovnikov, *Quench dynamics near a quantum critical point*, *Phys. Rev. B* **81** (2010) 012303. 11
- [12] A. Chandran, A. Erez, S.S. Gubser and S.L. Sondhi, *Kibble-zurek problem: Universality and the scaling limit*, *Physical Review B* **86** (2012) . 11
- [13] I. Kukuljan, S.c.v. Grozdanov and T.c.v. Prosen, *Weak quantum chaos*, *Phys. Rev. B* **96** (2017) 060301. 12
- [14] G. Gur-Ari, M. Hanada and S.H. Shenker, *Chaos in Classical D0-Brane Mechanics*, *JHEP* **02** (2016) 091 [1512.00019]. 13
- [15] E. Berkowitz, M. Hanada and J. Maltz, *Chaos in Matrix Models and Black Hole Evaporation*, *Phys. Rev. D* **94** (2016) 126009 [1602.01473]. 13

- [16] G. Mandal and T. Morita, *Quantum quench in matrix models: Dynamical phase transitions, Selective equilibration and the Generalized Gibbs Ensemble*, *JHEP* **10** (2013) 197 [1302.0859]. 13
- [17] E.B. Rozenbaum, S. Ganeshan and V. Galitski, *Lyapunov exponent and out-of-time-ordered correlator's growth rate in a chaotic system*, *Phys. Rev. Lett.* **118** (2017) 086801. 13
- [18] K. Hashimoto, K. Murata and R. Yoshii, *Out-of-time-order correlators in quantum mechanics*, *JHEP* **10** (2017) 138 [1703.09435]. 13
- [19] P. Basu and S.R. Das, *Quantum Quench across a Holographic Critical Point*, *JHEP* **01** (2012) 103 [1109.3909]. 13
- [20] S.H. Shenker and D. Stanford, *Black holes and the butterfly effect*, *JHEP* **03** (2014) 067 [1306.0622]. 13
- [21] T. Hartman and J. Maldacena, *Time Evolution of Entanglement Entropy from Black Hole Interiors*, *JHEP* **05** (2013) 014 [1303.1080]. 13
- [22] J.R. David, S. Khetrpal and S.P. Kumar, *Local quenches and quantum chaos from higher spin perturbations*, *JHEP* **10** (2017) 156 [1707.07166]. 13
- [23] T. Goldfriend and J. Kurchan, *Out-of-time-order correlator in weakly perturbed integrable systems*, 1911.04011. 14
- [24] M. Heyl, F. Pollmann and B. Dóra, *Detecting equilibrium and dynamical quantum phase transitions in ising chains via out-of-time-ordered correlators*, *Physical Review Letters* **121** (2018) . 14
- [25] S. Bandyopadhyay, A. Polkovnikov and A. Dutta, *Observing dynamical quantum phase transitions through quasilocal string operators*, *Physical Review Letters* **126** (2021) . 14
- [26] D. Das, “Quenched scramblings and symmetry.” [online notes](#), 08, 2021. 14
- [27] D. Ben-Zion and J. McGreevy, *Strange metal from local quantum chaos*, *Phys. Rev. B* **97** (2018) 155117 [1711.02686]. 14
- [28] M.C. Banuls, M.P. Heller, K. Jansen, J. Knaute and V. Svensson, *From spin chains to real-time thermal field theory using tensor networks*, *Phys. Rev. Res.* **2** (2020) 033301 [1912.08836]. 14
- [29] D. Chowdhury and B. Swingle, *Onset of many-body chaos in the $O(N)$ model*, *Phys. Rev. D* **96** (2017) 065005 [1703.02545]. 14
- [30] S.-K. Jian and H. Yao, *Universal properties of many-body quantum chaos at Gross-Neveu criticality*, 1805.12299. 14
- [31] S.R. Das and K. Sengupta, *Non-equilibrium Dynamics of $O(N)$ Nonlinear Sigma models: a Large- N approach*, *JHEP* **09** (2012) 072 [1202.2458]. 14

- [32] D. Das and B. Dey, *Quantum quench, large N, and symmetry restoration*, *JHEP* **07** (2020) 107 [[2003.11745](#)]. 14
- [33] J. Haegeman, J.I. Cirac, T.J. Osborne, I. Pižorn, H. Verschelde and F. Verstraete, *Time-dependent variational principle for quantum lattices*, *Physical review letters* **107** (2011) 070601. 15
- [34] T. Koffel, M. Lewenstein and L. Tagliacozzo, *Entanglement entropy for the long-range ising chain in a transverse field*, *Physical review letters* **109** (2012) 267203. 15
- [35] C. Lubich, T. Rohwedder, R. Schneider and B. Vandereycken, *Dynamical approximation by hierarchical tucker and tensor-train tensors*, *SIAM Journal on Matrix Analysis and Applications* **34** (2013) 470. 15
- [36] C. Hubig, I.P. McCulloch, U. Schollwöck and F.A. Wolf, *Strictly single-site dmrg algorithm with subspace expansion*, *Physical Review B* **91** (2015) 155115. 15
- [37] J. Haegeman, C. Lubich, I. Oseledets, B. Vandereycken and F. Verstraete, *Unifying time evolution and optimization with matrix product states*, *Physical Review B* **94** (2016) 165116. 15, 16
- [38] T. Chanda, P. Sierant and J. Zakrzewski, *Time dynamics with matrix product states: Many-body localization transition of large systems revisited*, *Physical Review B* **101** (2020) 035148. 16